Intervertebral Disc Health Preservation After Six Months of Spinal Growth Modulation

Vidyadhar V. Upasani, MD, Christine L. Farnsworth, MS, Reid C. Chambers, BA, Tracey P. Bastrom, MA, Gregory M. Williams, PhD, Robert L. Sah, MD, ScD, Koichi Masuda, MD, and Peter O. Newton, MD

Investigation performed at the Rady Children's Hospital and Health Center, San Diego, California

Background: Spinal growth modulation has been proposed as a non-fusion strategy for treatment of idiopathic scoliosis, although the effect of this treatment modality on intervertebral disc health has not been evaluated in detail. The objectives of this in vivo study were to assess the creation of three-dimensional spinal deformity during six months of growth modulation compared with that in sham-surgery controls, and to compare, with use of magnetic resonance imaging (MRI), gross morphological, histological, and biochemical analyses, disc health between control animals and animals treated with a spinal tether.

Methods: Six immature Yucatan mini-pigs underwent anterior spinal instrumentation with vertebral screws connected by a polyethylene tether over four consecutive thoracic vertebrae (T8-T11). An additional six animals underwent sham surgery (screw placement only [the control group]). Radiographs were obtained preoperatively, postoperatively, and monthly thereafter during six months of growth. Computed tomography (CT) and MRI studies were performed ex vivo, and the spines were sectioned for histological and biochemical analyses. Multivariate analysis of variance (MANOVA) was used to compare six-month postoperative data between the control and tethered animals, with the alpha level of significance set at 0.05.

Results: Radiographs and CT images demonstrated the creation of significant three-dimensional deformity ($p < 0.013$) in the tethered animals compared with the controls. Macroscopic, MRI, and histological evaluation revealed no signs of disc degeneration, with a bulging gelatinous nucleus pulposus, discrete fibrous anular lamellae, and uniformly hyperintense T2-signal intensity within the nuclei pulposi. Biochemical analysis demonstrated no significant difference in the nuclei pulposus between the tethered and control vertebrae; however, the water content ($p < 0.001$) of both sides of the anulus fibrosus and the glycosaminoglycan content ($p < 0.001$) of the left side of the anulus fibrosus differed significantly between the two groups.

Conclusions: Six months of spinal growth modulation created significant spinal deformity in all three planes compared with what was found in the sham-surgery controls. Although disc health was qualitatively maintained, quantitative changes in the anulus fibrosus water content and the disc height were observed on the side opposite to the tether. These changes likely represent metabolic responses of the discs to compressive loads generated by the flexible tether.

Clinical Relevance: Clinical trials are needed to evaluate the ability of an anterolateral spinal tether to correct deformity while preserving spinal flexibility and intervertebral disc health.

Idiopathic scoliosis is a common disorder of the pediatric spine that results in a three-dimensional deformity. Asymmetric spinal growth and biomechanical imbalance have been postulated as causes of this progressive deformity[1]. Although various treatment methods have been proposed, only bracing and surgical fusion affect the natural history of

Disclosure: One or more of the authors received payments or services, either directly or indirectly (i.e., via his or her institution), from a third party in support of an aspect of this work. In addition, one or more of the authors, or his or her institution, has had a financial relationship, in the thirty-six months prior to submission of this work, with an entity in the biomedical arena that could be perceived to influence or have the potential to influence what is written in this work. No author has had any other relationships, or has engaged in any other activities, that could be perceived to influence or have the potential to influence what is written in this work. The complete **Disclosures of Potential Conflicts of Interest** submitted by authors are always provided with the online version of the article.

idiopathic scoliosis compared with the deformity seen after observation alone[2,3]. However, even these two options have limitations. Bracing may prevent curve progression but generally affords little curve correction, despite optimal compliance[3,4], while surgical treatments sacrifice spinal flexibility to obtain and maintain curve correction. Ideally, a third option that would permanently straighten the spinal deformity while preserving spinal mobility and long-term function would be available.

Mechanical alteration of spinal growth by shortening the anterior vertebral column with an "internal brace" has been proposed as an attractive non-fusion treatment option for this multiplane deformity. Limiting anterior spinal overgrowth[5,6] has been considered since Blount and Clarke[7] and Haas[8] reported their initial work on epiphysiodesis in long bones. Recent studies on growth modulation in the axial skeleton have focused on retarding growth at the convexity of the deformity[9-13]. Use of an anterolateral flexible vertebral tether has also been shown to modulate spinal growth in animal models[14,15]. However, further evaluation of intervertebral disc health and spinal mobility is needed to determine if these techniques will be successful in the adolescent population.

The intervertebral disc is a flexible fibrocartilaginous structure that supports spinal loads while facilitating spinal movement. Disc degeneration has a multifactorial etiology, but decreased disc nutrition has been proposed as a common degenerative pathway, as the primary nutrition source for the avascular disc is diffusion from anular fibrosus and vertebral end-plate blood vessels[16]. Disc degeneration may develop prematurely secondary to compressive forces or it may occur as a result of natural aging leading to a breakdown of the large aggregating proteoglycans and loss of type-II collagen in the nucleus pulposus[16,17]. Decreased proteoglycans then reduce the capacity of the disc to attract and bind water, leading to a loss of hydration and decreased hydrostatic pressure[18]. Progressive disc degeneration leads to anular tears, rim lesions, decreased disc height, structural changes in the lamellar architecture of the anulus fibrosus, and formation of osteophytes.

Traditionally, biochemical analyses and the Thompson grading scale[19] have been used to characterize the state of disc degeneration. Pathomorphological and biochemical methods of grading intervertebral disc degeneration have been found to correlate well and are the gold standard for the analysis of cadaveric tissue. Differences in Thompson grades are reflected by changes in the concentration of disc constituents such as collagen and proteoglycans in both the anulus fibrosus and the nucleus pulposus. Clinically, magnetic resonance imaging (MRI) is the most sensitive and specific diagnostic tool for detection of disc degeneration.

The purpose of this study was to assess the creation of three-dimensional spinal deformity during six months of growth modulation compared with what was found in sham-surgery controls, and to compare disc health between tethered and control animals through use of MRI, gross morphological, histological, and biochemical analyses. We hypothesized that the spinal tether would create significant spinal deformity while preserving intervertebral disc health.

Materials and Methods

A seven-month-old male Yucatan mini-pig model, established previously[20], was used in this study, which was approved by the Institutional Animal Care and Use Committee. Sample size was based on a power analysis of previous data derived with use of this model for deformity creation (power = 0.8). Six animals underwent implantation of a flexible tether and grew for six months following tether application. Another six animals had sham surgery with implantation of vertebral body screws without placement of a tether, and they also grew for six months.

Surgical preparation, anesthesia, and postoperative care proceeded as reported previously[20]. A right thoracotomy was used for surgical exposure of the thoracic spine. No rib segments were removed. Instrumentation sites were prepared over four vertebral levels (T8-T11). Instrumentation was applied anterolaterally to each segment (on the right side) with one custom-designed vertebral staple and screw with a maximum outer diameter of 7.5 mm and a length of 35 mm (DePuy Spine, Raynham, Massachusetts). Neither discs nor growth plates were disturbed during implantation. In six animals, the vertebral body screws were aligned and an ultra-high molecular weight polyethylene (UHMWPE) ribbon tether (cross section, 1.5 × 7.5 mm) was placed and was fastened to the screws, connecting the four vertebrae (the tethered group). No tether was placed in the screws of the remaining six animals (the sham-surgery, or control, group).

Radiographs and Computed Tomography

Immediately prior to and following each operative procedure, biplanar (dorsoventral and lateral) spinal radiographs were obtained. During the six-month survival/growth period, biplanar radiographs of the spine were obtained monthly. After six months, all thoracic spines, including vertebral levels T7-T12, were harvested en bloc. Radiographic imaging was repeated following harvest. All radiographs were scanned, and digital measurements of the degree of scoliosis and sagittal alignment (the Cobb angle measured over the four instrumented levels) as well as vertebral body and disc wedging at each thoracic segment were performed with use of SpineView 2.4 software (Surgiview, Paris, France). Immediately following harvest, three-dimensional computed tomography (CT) scans of the fresh spines with the instrumentation in position were obtained. Vertebral body heights in the coronal (right versus left) and sagittal (anterior versus posterior) planes were measured for the four instrumented vertebrae (T8-T11) and two adjacent vertebrae (T7 and T12) as well as the three intervening discs (T8-T9, T9-T10, and T10-T11) and two adjacent discs (T7-T8 and T11-T12) with use of Amicas Vision Server Software (version 5.0; Amicas, Brighton, Massachusetts). Vertebral rotation was measured, with use of axial plane CT images, as the angle formed between a vertical line bisecting the vertebral body/spinous process and the true horizontal. Rotation of the T12 vertebral body was used as a baseline, with the rotation of the other vertebral bodies reported in comparison with that of T12.

MRI

Following CT scanning, all screws and tethers were removed to minimize artifact, and 3-T MRI scans were obtained with a GE Signa EXCITE scanner (GE Healthcare Technologies, Waukesha, Wisconsin), with M5 software. Qualitative evaluation of the MRI images included identification of osteophytes, disc extension beyond the interspace, the shape of the nucleus pulposus, the presence of anulus fibrosus tears, end-plate cartilage irregularities, the presence of Schmorl nodes, changes in T2-signal intensity, and changes in signal intensity in the vertebral body marrow next to the end plate.

Histological and Biochemical Analyses

The spines were wrapped in saline-solution-soaked towels and frozen at −20°C. Individual motion segments were isolated to include a disc with half

TABLE I Coronal Cobb Angle Measurements in the Control and Tethered Groups

	Control Group* (N = 6) *(deg)*	Tethered Group* (N = 6) *(deg)*	P Value
Preoperative	0.0 ± 0.4	−0.7 ± 0.5	0.65
Postoperative	2.2 ± 0.3	7.4 ± 0.7	0.09
1 month	0.3 ± 0.5	5.7 ± 0.5	0.011
2 months	1.8 ± 0.5	8.8 ± 0.7	0.008
3 months	3.7 ± 0.6	12.3 ± 0.6	0.003
4 months	4.2 ± 0.6	13.2 ± 0.7	0.003
5 months	2.5 ± 0.6	13.3 ± 1.2	0.007
6 months	4.5 ± 0.7	13.3 ± 1.0	0.013

*The values are given as the mean and standard error of the mean.

the adjacent vertebral body from either side. Three motion segments were obtained from each spine, for a total of eighteen discs from the tethered group and eighteen from the sham-surgery group. Each motion segment was divided through the coronal midline of the vertebral body, resulting in an anterior and a posterior portion. High-resolution digital photographs of each disc were obtained, and the Thompson grading scale was used to assign a gross morphological grade to each intervertebral disc from T8 through T11[21].

For each isolated motion segment, one-half of the specimen (alternating between anterior and posterior) was placed in formalin to undergo histological processing and the other half was dissected to obtain tissue plugs for biochemical analysis. The motion segments preserved in formalin underwent histological analysis to evaluate for signs of degeneration and the effects of dynamic compression by using a previously described histological grading scale (see Appendix)[22]. For the biochemical analysis, four plugs were obtained with 11-gauge Jamshidi needles from each frozen disc: from the right and left sides of the anulus fibrosus and the right and left sides of the nucleus pulposus. Wet weights and dry weights following lyophilization were obtained to determine the percentage water content for each plug. Tissue digests were assessed for DNA with PicoGreen (Invitrogen, Carlsbad, California)[23], for glycosaminoglycans with dimethylmethylene blue[24], and for hydroxyproline with dimethylaminobenzaldehyde[25]. Subsequently, cell content was determined with use of a ratio of 7.7 pg of DNA per cell[26], and an index of collagen content was determined with use of a ratio of 7.25 g of collagen per gram of hydroxyproline[27,28]. These concentrations were compared between the right and left sides of the anulus fibrosus and between the right and left sides of the nucleus pulposus for each group and between the control and tethered surgical groups.

Statistical Analysis

Continuous data were screened for normality with use of the normal Q-Q plot of the residuals. If the distribution looked questionable, a more formal check of normality, the one-sample Kolmogorov-Smirnov statistic, was calculated. The Levene test for homogeneity of variance was also performed prior to application of parametric testing. Repeated-measures analysis of variance (ANOVA), with the presence or absence of a tether as the between-subjects factor, was utilized to evaluate changes in radiographic measures over time. Subsequently, a series of multivariate analyses of variance (MANOVA) were used to evaluate between-group differences in the radiographic measures at individual time points, with the presence or absence of a tether as the independent variable. The alpha level for significance was set at 0.05. Categorical dependent variables were analyzed for proportional differences between the

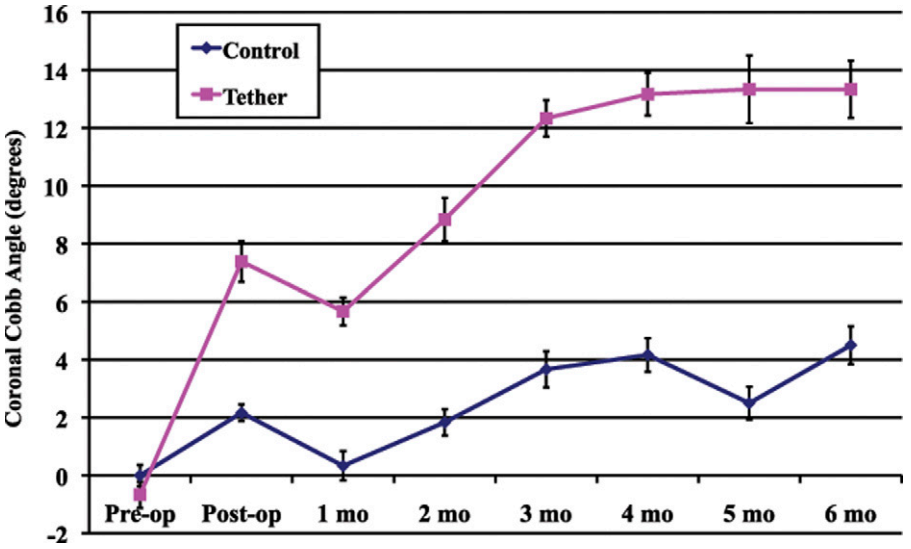

Fig. 1

Coronal Cobb angle measurements (average and standard error of the mean) over the six-month survival period in the sham-surgery control and tethered groups.

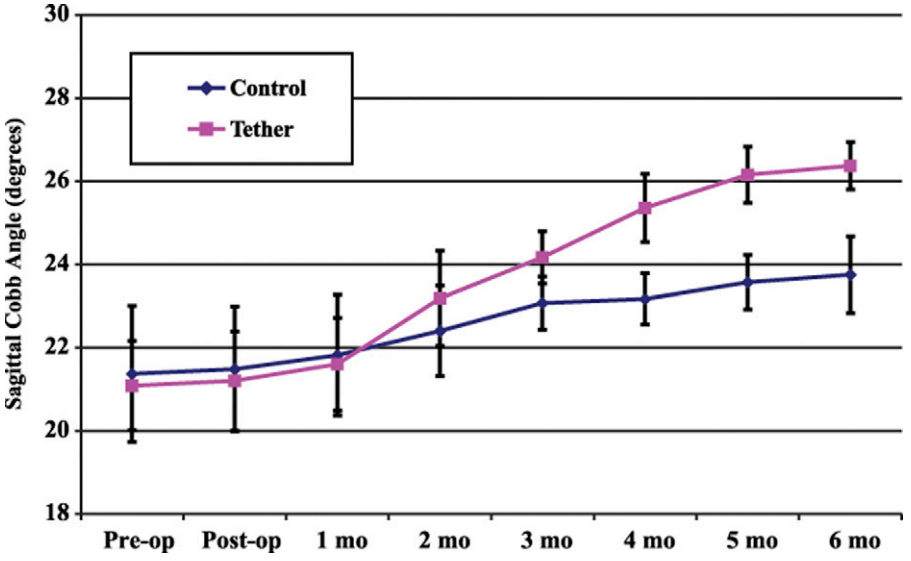

Fig. 2
Sagittal Cobb angle measurements (average and standard error of the mean) over the six-month survival period in the sham-surgery control and tethered groups.

two study groups with use of cross tabulation and the chi-square statistic ($p < 0.05$).

Source of Funding
Funding for this study was provided by a research grant from the Association of Bone and Joint Surgeons and the Orthopaedic Research and Education Foundation. Additional financial support was provided by the Rady Children's Specialists Foundation. The implants were provided by DePuy Spine at no cost to the investigators.

Results

Preoperatively, the two surgical groups had similar body weights (mean and standard deviation, 26.8 ± 1.6 and 26.2 ± 2.4 kg, $p = 0.66$) and body lengths (76.9 ± 3.0 and 76.2 ± 2.1 cm, $p = 0.61$). Intraoperative blood loss and surgical time were also similar in the two groups ($p = 0.75$ and $p = 0.62$, respectively).

Radiographic Measurements
There were no significant differences between the two surgical groups with respect to either the preoperative or the immediate postoperative coronal Cobb angles; however, every subsequent postoperative radiograph demonstrated significantly greater deformity in the tethered group (Table I). Figures 1 and 2 demonstrate the average coronal and sagittal Cobb angles in the two groups over the six-month survival period. The animals in the tethered group developed a greater thoracic kyphosis over time, compared with that developed by the control animals, demonstrating a sagittal plane effect of the tether.

Vertebral body wedging was measured for the four tethered vertebrae (T8-T11) and for the two adjacent vertebrae (T7 and T12). In the tethered group (Fig. 3), the four tethered vertebrae became wedged after two months of growth. This deformity was most obvious in the two apical vertebrae of the

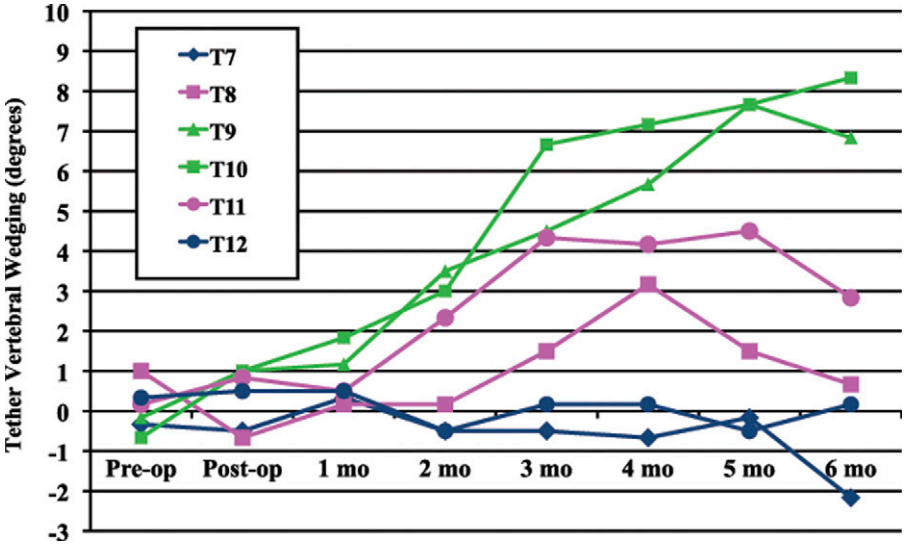

Fig. 3
Average coronal vertebral body wedging over the six-month survival period in the tethered group.

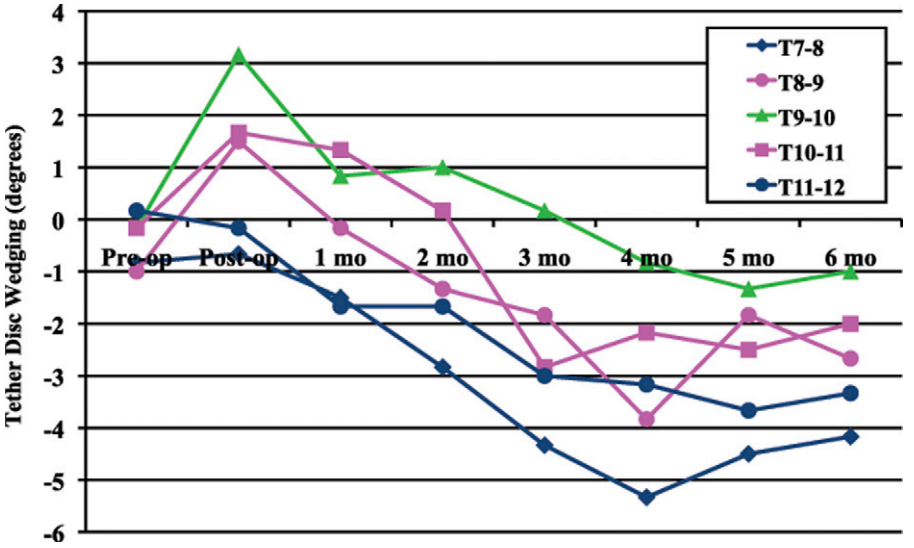

Fig. 4

Average coronal intervertebral disc wedging over the six-month survival period in the tethered group.

four-level instrumentation. The vertebral body wedging of all tethered vertebrae continued throughout the six-month growth period. At six months, there was an average (and standard error of the mean) of 0.7° ± 1.6° of vertebral body wedging at T8, 6.8° ± 4.4° at T9, 8.3° ± 3.5° at T10, and 2.8° ± 2.9° at T11.

Intervertebral disc wedging was measured at the three tethered levels (T8-T9, T9-T10, and T10-T11) and at the two adjacent levels (T7-T8 and T11-T12). Minimal intervertebral disc wedging was observed in the control group. Immediately postoperatively, the discs at the tethered levels were wedged, with a higher disc height on the left side (away from the tether) than on the right (tethered) side ("positive angulation" of 1.5° ± 1.8° at T8-T9, 3.2° ± 2.4° at T9-10, and 1.7° ± 2.3° at T10-T11) (Fig. 4). By six months postoperatively, however, the discs had developed reverse wedging (a higher disc height on the tethered side, with "negative angulation" of −2.7° ± 1.4° at T8-T9, −1.0° ± 1.8° at T9-T10, and −2.0° ± 1.3° at T10-T11). This transition occurred between the second and third

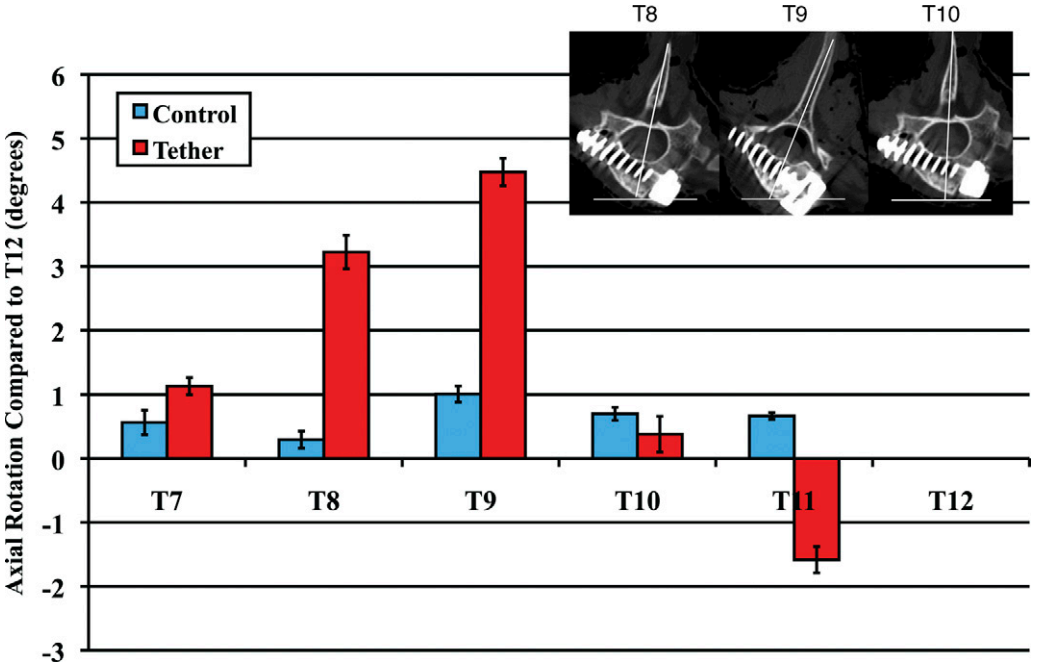

Fig. 5

Deformity creation in the axial plane—i.e., vertebral body rotation (average and standard error of the mean) with respect to that at T12—in the sham-surgery control and tethered groups.

postoperative months, correlating with the developing vertebral body wedging.

CT

CT measurements of vertebral body and disc heights confirmed the radiographic findings at six months postoperatively. The flexible spinal tether created a substantial difference in vertebral body height between the right and left sides and between the anterior and posterior aspects. These results demonstrate the ability of the tether to slow axial growth on the side of the tether (right or anterior). No significant difference in vertebral height was found between the control and tethered groups (T7-T12) in either plane ($p > 0.14$).

Disc height was affected by the spinal tether. In the coronal plane, the discs in the tethered group increased in height on the right side of the spine (opposite from the vertebral body growth and toward the tether). In the sagittal plane, the discs increased in height on the anterior aspect of the spine (again, opposite from the vertebral body growth and toward the tether). Of note, in the sagittal plane, the tethered discs were significantly more narrowed on average compared with the control discs ($p = 0.001$).

Measurements on the axial CT images showed no significant creation of axial plane deformity in the control animals (Fig. 5). In the tethered group, T8 and T9 were noted to be significantly more rotated than the adjacent vertebral bodies ($p \leq 0.008$). This rotation was most evident at T9, which appeared to be the apex of the rotational deformity created with a four-level anterolateral tether instrumentation construct.

MRI

Figure 6 demonstrates mid-coronal 3-T MRI T1-weighted and T2-weighted images of a representative animal from each group. Qualitative evaluation[29] demonstrated no evidence of osteophytes, disc extension beyond the interspace, anular tears, end-plate cartilage irregularities, or Schmorl nodes in any of the instrumented or sham-operation discs. Of note, one sham-operation disc was found to have intranuclear fibrosis of unknown etiology.

Histological and Biochemical Analysis

All but one disc were given a Thompson grade of 1, indicating a bulging gelatinous nucleus pulposus with discrete fibrous lamellae in the anulus fibrosus. The exception was one control disc (as noted on MRI), which was given a grade of 3 as there appeared to be some consolidated fibrous tissue in the nucleus.

On the basis of the grading system in the Appendix[22], the average grade for the control discs was 5.3 ± 1.2 points. This included the one disc with internuclear fibrosis, which received a grade of 8 points. The average grade for the discs in the tethered group was 5.6 ± 1.0 points. None of the discs in the tethered group scored >7 points. Although the average score in the tethered group was slightly higher than that in the control group, this difference was not significant ($p = 0.38$).

The biochemical data are shown in Table II. In the control group, the nucleus pulposus water content was 87.5% ± 0.7% on the right side and 85.5% ± 0.8% on the left side. In the tethered group, the water contents on the right and left sides were 84.4% ± 1.1% and 86.0 ± 0.9%, respectively. A two-way ANOVA showed no difference between the water content of the nucleus pulposus in the control group and that in the tethered group ($p = 0.11$) or between the water contents on the right and left sides ($p = 0.92$), with an interaction term of $p = 0.14$.

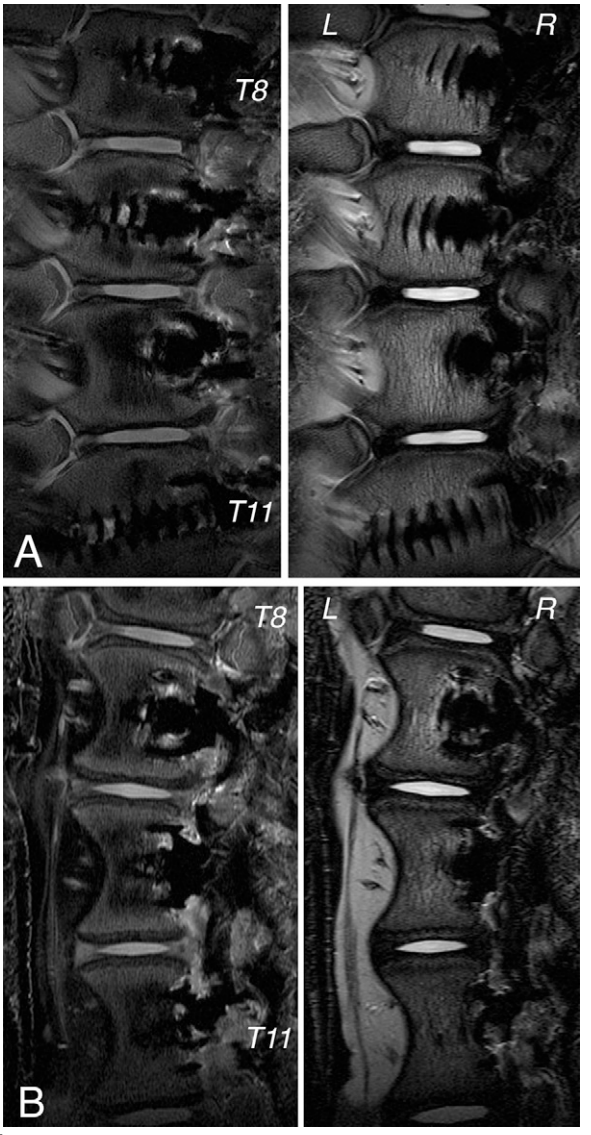

Fig. 6

Representative mid-coronal 3-T MRI images (T1-weighted on the left and T2-weighted on the right) acquired six months postoperatively in the sham-surgery control (A) and tethered (B) groups.

The anulus fibrosus had a lower water content than did the nucleus pulposus, with the control group having an anulus water content of 66.9% ± 0.8% on the right side and 68.8% ± 1.5% on the left side. In the tethered group, the anulus water contents on the right and left sides were 61.0% ± 1.4% and 58.1% ± 1.7%, respectively. A two-way ANOVA showed a significant difference in the anulus water content between the tethered and control

TABLE II Biochemical Data in the Control and Tethered Groups*

	Water Content *(%)*	Glycosaminoglycan Content *(% wet weight)*	Hydroxyproline Content *(% wet weight)*	Cell Count *(10^6 cells/g dry weight)*
Control group†				
Right side of anulus fibrosus	66.9 ± 0.8	2.3 ± 0.3	2.8 ± 0.2	170 ± 20
Right side of nucleus pulposus	87.5 ± 0.7	7.2 ± 0.4	0.14 ± 0.04	380 ± 20
Left side of nucleus	85.5 ± 0.8	8.3 ± 0.5	0.44 ± 0.16	320 ± 20
Left side of anulus fibrosus†	68.8 ± 1.5	4.4 ± 0.3	2.5 ± 0.2	140 ± 10
Tethered group†				
Right side of anulus fibrosus	61.0 ± 1.4	2.7 ± 0.5	2.8 ± 0.3	140 ± 20
Right side of nucleus pulposus	84.4 ± 1.1	7.3 ± 0.6	0.41 ± 0.01	390 ± 30
Left side of nucleus pulposus	86.0 ± 0.9	7.3 ± 0.6	0.22 ± 0.17	380 ± 20
Left side of anulus†	58.1 ± 1.7	2.8 ± 0.3	2.8 ± 0.3	150 ± 10

*The values are given as the mean and standard error of the mean. †A significant difference in water content in the anulus fibrosus was found between the control and tethered groups ($p < 0.001$). ‡A significant difference in glycosaminoglycan content in the left side of the anulus was found between the control and tethered groups ($p < 0.001$).

groups ($p < 0.001$), but no difference between the right and left sides ($p = 0.71$), with an interaction term of $p = 0.87$. A significant difference in the glycosaminoglycan content in the left side of the anulus was found between the control (4.4% ± 0.3%) and tethered (2.8% ± 0.3%) groups ($p < 0.001$). Hydroxyproline content and cell-density data are presented in Table II, with no significant differences found between the control and tethered groups or between the right and left sides.

Discussion

The vertebral staple-screw-tether construct used in this study consistently modulated spinal growth, resulting in the creation of a three-dimensional spinal deformity. Deformity creation was followed radiographically throughout the six-month study period and then after spine harvest. CT was used to further define the effect of the tether on vertebral body and intervertebral disc morphology.

As expected, the vertebral bodies did not change in shape during the surgical procedure. It was not until approximately two months after the surgery that a change in the shape of the vertebral bodies was observed (Fig. 3). From that time, the tethered vertebral bodies became increasingly wedged (Fig. 4) away from the tether (increased left-sided height). These findings are similar to those reported previously in studies of spinal growth modulation[13,14,20] We assume that this change in shape is caused by a slowing of endochondral ossification on the side of the tether (the right side). Mechanical compression of the growth plate, either generated actively during the surgical procedure by manual tensioning of the spinal tether or generated by the increasing length of the spine (passive growth related tensioning of the tether), appears to be responsible for observed changes in vertebral body shape. Future studies focusing on the effect of compression on the physeal cartilage of vertebrae are needed.

Axial plane deformity was also observed on the six-month CT images (Fig. 5). It is possible that this deformity occurred over time as the vertebral bodies became increasingly wedged; however, we were not able to quantify axial deformity from the monthly radiographs. Dickson proposed that the axial plane deformity observed in idiopathic scoliosis was due to an imbalance in the heights of the anterior and posterior columns of the spine[1]. Similarly, the imbalance in vertebral body height may have caused the porcine spines in our study to rotate laterally, although no monthly CTs were obtained. It is clear, however, that there was more rotation in the tethered spines than there was in the control spines at the six-month postoperative time point.

In terms of the intervertebral discs, one would assume that, once the discs are wedged away from the tether immediately postoperatively, compression from the spinal tether would cause the discs to remain wedged in that direction. This was not the case. By two months postoperatively, the discs were no longer wedged; at approximately three months postoperatively, they started to become wedged toward the tether (the disc height on the tethered, right side was increased compared with that on the left side [Fig. 4]). Additionally, at six months postoperatively, CT analysis showed the discs in the tethered group to be significantly more narrowed than those in the controls. Previous studies of alternate techniques of spinal growth modulation have not demonstrated this phenomenon of reverse disc wedging[12,13]; however, we had observed these findings previously with the flexible spinal tether[20] and wanted to evaluate what was happening within the discs in more detail. The control group allowed us to evaluate the isolated effect of the spinal tether on the intervertebral discs.

The viability of the discs is a critical component in the development of this treatment modality as a fusionless correction for idiopathic scoliosis. If the discs do not remain healthy after experiencing a compressive load for a prolonged period of time, motion preservation after removal of the tether is unlikely. We hypothesized that the flexible UHMWPE tether would

produce a dynamic compression that would affect physeal growth while preserving disc health. Since the introduction of fast-spin-echo imaging in the early 1990s[30], MRI technology has advanced the ability to detect early signs of disc degeneration. Pfirrmann et al. developed a comprehensive MRI grading system based on the gross morphology of the degeneration of the lumbar intervertebral disc as seen on routine T2-weighted MRIs[29]. Vertebral end plate changes, such as sclerosis, Schmorl nodes, and other irregularities, were found to occur prior to disc degeneration and were seen on radiographs and MRIs[31,32]. Modic et al. noticed signal intensity changes in the vertebral body marrow adjacent to the end plate and associated them with clinical symptoms related to degenerative disc disease[33,34].

Signal characteristics of the disc on T2-weighted MRIs reflect changes caused by aging and/or late-stage degenerative changes, including changes in disc morphology, height, hydration, bulging, and herniation[35]. Intervertebral disc degeneration is inferred from the findings of reduced T2-signal intensity, reduced disc height, and/or the presence of fissures. The signal intensity in the nucleus pulposus of normal intervertebral discs has been shown to correlate directly with the proteoglycan concentration[36]. MRI findings of disc degeneration increase the accuracy of the gross morphological grading systems; however, degenerative states could be more effectively and quantitatively measured with a method based on measurement of the chemical constituents of the disc through the use of biochemical techniques.

In general, obvious disc degeneration was not present at any level in either the tethered or the control group. One control disc had a central area with low T2-signal intensity, which was found to be fibrotic tissue. It is not clear whether we somehow damaged the disc, causing it to become fibrotic, or if the fibrotic tissue was an anatomic anomaly in that animal. Radiographs did not demonstrate the lesion, and we did not have preoperative CT or MRI images of that animal to evaluate the disc. The anatomic dissection demonstrated that the tines of the vertebral staple had not penetrated into the disc, and there were no overlying osteophytes or other signs of degeneration present at that level.

The biochemical changes due to tethering are consistent with a physiological response to compression and a healthy disc. No significant differences in the average water content, glycosaminoglycan content, or cell density in the nucleus pulposus were found between the tethered and control groups. The water content in the anulus fibrosus, however, was decreased significantly in the tethered group compared with that in the controls. This decrease in water content may have been responsible for the loss of disc height observed in the sagittal CT analysis. Histological analysis, however, did not demonstrate a disruption in the fibers of the anular fibrocartilage. This finding is consistent with the absence of disc degeneration in the anulus or is possibly a sign of very early-stage degeneration. There were no differences between the right and left sides of the tethered vertebral bodies. While the interaction between tethered/control group and left/right side for water content was not significant, there was insufficient power for these statistical comparisons (below 40% for both). With the magnitude of the effect (eta = 0.19) approaching what would be considered a medium effect size (0.25), it is estimated that sixty-five samples per group would be required to reach an alpha of 0.05.

The preservation of the nucleus pulposus, in terms of water and glycosaminoglycan content and cell density, in the tethered group was reassuring. Our current knowledge of intervertebral disc degeneration seems to indicate that a loss of water content in the nucleus pulposus is one of the earliest signs of disc degeneration, and the loss of water is a direct result of proteoglycan breakdown[16-18,21,37,38]. As the nucleus pulposus loses its capacity to resist compression, the surrounding anular structure breaks down and the disc loses its structure and function[16]. In the tethered group, there was a definite change in disc shape, without any measurable changes in the composition of the nucleus pulposus. This may indicate that the nucleus pulposus is physiologically responding to the compression generated by the tether and is not degenerating, at least at the six-month time point. Despite this knowledge, numerous questions remain. Future studies are needed to evaluate molecular markers of disc degeneration such as matrix metalloproteinases (MMPs) as well as catabolic cytokines, changes in collagen typing, and oxygen tension in the nucleus[39].

The data obtained from this study have the potential to directly impact patient care and promote the development of an "internal brace" for the treatment of idiopathic scoliosis. The anterolateral flexible tether is ideally suited for the treatment of juvenile scoliosis, as these children have many years of growth potential and have a well-described risk of curve progression. Children with juvenile scoliosis of >30° have a 100% chance of curve progression and a 100% need for surgical treatment[40]. If an "internal brace" were used early in this patient population, it might help to control the curve and possibly avoid spinal instrumentation and fusion. For the anterolateral flexible tether to be a viable option as an "internal brace," it has to be able to modulate spinal growth without affecting spinal mobility or disc health.

Several limitations of this study and the porcine model have to be considered when these data are evaluated. Primarily, differences in spinal mechanical forces secondary to postural differences between a quadruped pig and a bipedal human may affect the ability to modulate growth. The evaluation of disc health was performed in this study after only six months of growth modulation, while these tethers would be in place in adolescents for several years before the patients reached skeletal maturity. The effect of a long-term compressive load and motion limitation on disc health will need to be studied in the future. Finally, this is an animal model that creates deformity rather than corrects it. As such, it is unclear exactly to what extent such a growth modulating approach will be successful in arresting or correcting progressive scoliosis in a growing child or adolescent. If these growth effects on a nonscoliotic pig translate to humans, the outlook for the treatment of scoliosis may change substantially.

Appendix

eA An appendix showing the histological grading scale is available with the online version of this article at jbjs.org. ■

NOTE: The authors recognize Graeme M. Bydder, MB, ChB, for generous insight regarding MRI analysis; Richard Znamirowski, RT, for MRI acquisition and processing; David Andrews, RT, for CT acquisition and processing; and Eric Breisch, PhD, for histological processing and analysis.

Vidyadhar V. Upasani, MD
Koichi Masuda, MD
Department of Orthopaedic Surgery,
University of California at San Diego,
350 Dickenson Street, MC 8894,
San Diego, CA 92103

Christine L. Farnsworth, MS
Reid C. Chambers, BA
Tracey P. Bastrom, MA
Peter O. Newton, MD
Department of Orthopedic Surgery,
Rady Children's Hospital and Health Center at San Diego,
3030 Children's Way, Suite 410,
San Diego, CA 92123.
E-mail address for P.O. Newton: pnewton@rchsd.org

Gregory M. Williams, PhD
Robert L. Sah, MD, ScD
Department of Bioengineering,
University of California at San Diego,
9500 Gilman Drive, MC 0412,
La Jolla, CA 92093

References

1. Dickson RA. Aetiology of idiopathic spinal deformities. Arch Dis Child. 1985;60:508-11.
2. Dickson RA, Weinstein SL. Bracing (and screening)—yes or no? J Bone Joint Surg Br. 1999;81:193-8.
3. Nachemson AL, Peterson LE. Effectiveness of treatment with a brace in girls who have adolescent idiopathic scoliosis. A prospective, controlled study based on data from the Brace Study of the Scoliosis Research Society. J Bone Joint Surg Am. 1995;77:815-22.
4. Goldberg CJ, Dowling FE, Hall JE, Emans JB. A statistical comparison between natural history of idiopathic scoliosis and brace treatment in skeletally immature adolescent girls. Spine (Phila Pa 1976). 1993;18:902-8.
5. Guo X, Chau WW, Chan YL, Cheng JC. Relative anterior spinal overgrowth in adolescent idiopathic scoliosis. Results of disproportionate endochondral-membranous bone growth. J Bone Joint Surg Br. 2003;85:1026-31.
6. Dickson RA, Lawton JO, Archer IA, Butt WP. The pathogenesis of idiopathic scoliosis. Biplanar spinal asymmetry. J Bone Joint Surg Br. 1984;66:8-15.
7. Blount WP, Clarke GR. The classic. Control of bone growth by epiphyseal stapling. A preliminary report. Journal of Bone and Joint Surgery, July, 1949. Clin Orthop Relat Res. 1971;77:4–17.
8. Haas SL. Mechanical retardation of bone growth. J Bone Joint Surg Am. 1948;30:506-12.
9. Smith AD, Von Lackum WH, Wylie R. An operation for stapling vertebral bodies in congenital scoliosis. J Bone Joint Surg Am. 1954;36:342-8.
10. Piggott H. Growth modification in the treatment of scoliosis. Orthopedics. 1987;10:945-52.
11. Roaf R. Vertebral growth and its mechanical control. J Bone Joint Surg Br. 1960;42:40-59.
12. Betz RR, D'Andrea LP, Mulcahey MJ, Chafetz RS. Vertebral body stapling procedure for the treatment of scoliosis in the growing child. Clin Orthop Relat Res. 2005;434:55-60.
13. Braun JT, Hoffman M, Akyuz E, Ogilvie JW, Brodke DS, Bachus KN. Mechanical modulation of vertebral growth in the fusionless treatment of progressive scoliosis in an experimental model. Spine (Phila Pa 1976). 2006;31:1314-20.
14. Newton PO, Faro FD, Farnsworth CL, Shapiro GS, Mohamad F, Parent S, Fricka K. Multilevel spinal growth modulation with an anterolateral flexible tether in an immature bovine model. Spine (Phila Pa 1976). 2005;30:2608-13.
15. Newton PO, Fricka KB, Lee SS, Farnsworth CL, Cox TG, Mahar AT. Asymmetrical flexible tethering of spine growth in an immature bovine model. Spine (Phila Pa 1976). 2002;27:689-93.
16. Buckwalter JA. Aging and degeneration of the human intervertebral disc. Spine 1995;20:1307-14.
17. Pearce RH, Grimmer BJ, Adams ME. Degeneration and the chemical composition of the human lumbar intervertebral disc. J Orthop Res. 1987;5:198-205.
18. Antoniou J, Steffen T, Nelson F, Winterbottom N, Hollander AP, Poole RA, Aebi M, Alini M. The human lumbar intervertebral disc: evidence for changes in the biosynthesis and denaturation of the extracellular matrix with growth, maturation, ageing, and degeneration. J Clin Invest. 1996;98:996-1003.
19. Thompson JP, Pearce RH, Schechter MT, Adams ME, Tsang IK, Bishop PB. Preliminary evaluation of a scheme for grading the gross morphology of the human intervertebral disc. Spine (Phila Pa 1976). 1990;15:411-5.
20. Newton PO, Upasani VV, Farnsworth CL, Oka R, Chambers RC, Dwek J, Kim JR, Perry A, Mahar AT. Spinal growth modulation with use of a tether in an immature porcine model. J Bone Joint Surg Am. 2008;90:2695-706.
21. Benneker LM, Heini PF, Anderson SE, Alini M, Ito K. Correlation of radiographic and MRI parameters to morphological and biochemical assessment of intervertebral disc degeneration. Eur Spine J. 2005;14:27-35.
22. Han B, Zhu K, Li FC, Xiao YX, Feng J, Shi ZL, Lin M, Wang J, Chen QX. A simple disc degeneration model induced by percutaneous needle puncture in the rat tail. Spine (Phila Pa 1976). 2008;33:1925-34.
23. McGowan KB, Kurtis MS, Lottman LM, Watson D, Sah RL. Biochemical quantification of DNA in human articular and septal cartilage using PicoGreen and Hoechst 33258. Osteoarthritis Cartilage. 2002;10:580-7.
24. Farndale RW, Buttle DJ, Barrett AJ, Farndale RW. Biochim Biophys Acta. 1986;883:173-7.
25. Woessner JF Jr. The determination of hydroxyproline in tissue and protein samples containing small proportions of this imino acid. Arch Biochem Biophys. 1961;93:440-7.
26. Kim YJ, Sah RL, Doong JY, Grodzinsky AJ. Fluorometric assay of DNA in cartilage explants using Hoechst 33258. Anal Biochem. 1988;174:168-76.
27. Herbage D, Bouillet J, Bernengo JC. Biochemical and physiochemical characterization of pepsin-solubilized type-II collagen from bovine articular cartilage. Biochem J. 1977;161:303-12.
28. Pal S, Tang LH, Choi H, Habermann E, Rosenberg L, Roughley P, Poole AR. Structural changes during development in bovine fetal epiphyseal cartilage. Collagen Relat Res. 1981;1:151-76.
29. Pfirrmann CW, Metzdorf A, Zanetti M, Hodler J, Boos N. Magnetic resonance classification of lumbar intervertebral disc degeneration. Spine (Phila Pa 1976). 2001;26:1873-8.
30. Listerud J, Einstein S, Outwater E, Kressel HY. First principles of fast spin echo. Magn Reson Q. 1992;8:199-244.
31. Hamanishi C, Kawabata T, Yosii T, Tanaka S. Schmorl's nodes on magnetic resonance imaging. Their incidence and clinical relevance. Spine (Phila Pa 1976). 1994;19:450-3.
32. Katz ME, Teitelbaum SL, Gilula LA, Resnick D, Katz SJ. Radiologic and pathologic patterns of end-plate-based vertebral sclerosis. Invest Radiol. 1988;23:447-54.
33. Modic MT, Masaryk TJ, Ross JS, Carter JR. Imaging of degenerative disk disease. Radiology. 1988;168:177-86.
34. Modic MT, Steinberg PM, Ross JS, Masaryk TJ, Carter JR. Degenerative disk disease: assessment of changes in vertebral body marrow with MR imaging. Radiology. 1988;166(1 Pt 1):193-9.
35. Morgan S, Saifuddin A. MRI of the lumbar intervertebral disc. Clin Radiol. 1999;54:703-23.
36. Pearce RH, Thompson JP, Bebault GM, Flak B. Magnetic resonance imaging reflects the chemical changes of aging degeneration in the human intervertebral disk. J Rheumatol Suppl. 1991;27:42-3.
37. Kääpä E, Holm S, Han X, Takala T, Kovanen V, Vanharanta H. Collagens in the injured porcine intervertebral disc. J Orthop Res. 1994;12:93-102.
38. Kääpä E, Holm S, Inkinen R, Lammi MJ, Tammi M, Vanharanta H. Proteoglycan chemistry in experimentally injured porcine intervertebral disk. J Spinal Disord. 1994;7:296-306.
39. Podichetty VK. The aging spine: the role of inflammatory mediators in intervertebral disc degeneration. Cell Mol Biol (Noisy-le-grand). 2007;53:4-18.
40. Charles YP, Daures JP, de Rosa V, Diméglio A, Charles YP, Daures JP, de Rosa V, Diméglio A. Spine (Phila Pa 1976). 2006;31:1933-42.